Cell Metabolism
Article

Divalent Metal Transporter 1 Regulates Iron-Mediated ROS and Pancreatic β Cell Fate in Response to Cytokines

Jakob Bondo Hansen,[1,15] Morten Fog Tonnesen,[5,15] Andreas Nygaard Madsen,[2] Peter H. Hagedorn,[6] Josefine Friberg,[3] Lars Groth Grunnet,[5] R. Scott Heller,[7] Anja Østergren Nielsen,[5] Joachim Størling,[8] Luc Baeyens,[9] Leeat Anker-Kitai,[10] Klaus Qvortrup,[4] Luc Bouwens,[9] Shimon Efrat,[10] Mogens Aalund,[11] Nancy C. Andrews,[12] Nils Billestrup,[3] Allan E. Karlsen,[5,13] Birgitte Holst,[2] Flemming Pociot,[8,13] and Thomas Mandrup-Poulsen[1,14,*]

[1]Center for Medical Research Methodology, Department of Biomedical Sciences
[2]Rodent Metabolic Phenotyping Center
[3]Department of Biomedical Sciences
[4]Core Facility for Integrated Microscopy, Department of Biomedical Sciences
University of Copenhagen, 2200 Copenhagen, Denmark
[5]Diabetes Biology and Hagedorn Research Institute, Novo Nordisk, 2820 Gentofte, Denmark
[6]Biosystems Department, Risø National Laboratory, Technical University of Denmark, 4000 Roskilde, Denmark
[7]Imaging Team, Novo Nordisk, 2760 Måløv, Denmark
[8]Glostrup Research Institute, Glostrup Hospital, 2600 Glostrup, Denmark
[9]Diabetes Research Center, Vrije Universiteit Brussel-Free University of Brussels, 1090 Brussels, Belgium
[10]Department of Human Molecular Genetics and Biochemistry, Sackler School of Medicine, Tel Aviv University, 69978 Tel Aviv, Israel
[11]Neurotech A/S, 2200 Copenhagen, Denmark
[12]Department of Pediatrics and Pharmacology and Department of Cancer Biology, Duke University School of Medicine, Durham, NC 27710, USA
[13]Clinical Research Center, University of Lund, 205 02 Malmö, Sweden
[14]Department of Molecular Medicine and Surgery, Karolinska Institutet, 171 77 Stockholm, Sweden
[15]These authors contributed equally to this work
*Correspondence: tmpo@sund.ku.dk
http://dx.doi.org/10.1016/j.cmet.2012.09.001

SUMMARY

Reactive oxygen species (ROS) contribute to target-cell damage in inflammatory and iron-overload diseases. Little is known about iron transport regulation during inflammatory attack. Through a combination of in vitro and in vivo studies, we show that the proinflammatory cytokine IL-1β induces divalent metal transporter 1 (DMT1) expression correlating with increased β cell iron content and ROS production. Iron chelation and siRNA and genetic knockdown of DMT1 expression reduce cytokine-induced ROS formation and cell death. Glucose-stimulated insulin secretion in the absence of cytokines in *Dmt1* knockout islets is defective, highlighting a physiological role of iron and ROS in the regulation of insulin secretion. *Dmt1* knockout mice are protected against multiple low-dose streptozotocin and high-fat diet-induced glucose intolerance, models of type 1 and type 2 diabetes, respectively. Thus, β cells become prone to ROS-mediated inflammatory damage via aberrant cellular iron metabolism, a finding with potential general cellular implications.

INTRODUCTION

Inflammation and oxidative stress contribute to the pathophysiology of the grand global health challenges: diabetes, cancer, neurodegenerative disorders, hypertension, and cardiovascular diseases. Inflammatory generation of reactive oxygen species (ROS) depends on the Fenton reaction catalyzed by redox-active metals, of which iron predominates. Iron overload causes oxidative stress and subsequent mitochondrial and DNA damage, lipid peroxidation, and protein modification, leading in particular to dysfunction of metabolically highly active cells, e.g., cardiomyocytes, hepatocytes, pituitary cells, chondrocytes, and pancreatic β cells (Eaton and Qian, 2002; Hamazaki et al., 1986; Jomova and Valko, 2011; Witzleben, 1966).

Proinflammatory cytokines generated by islet-infiltrating immune cells in type 1 and 2 diabetes are believed to impair β cell function and viability, in part via ROS formation, to which β cells are exquisitely sensitive due to inadequate antioxidative defense (Donath et al., 2008; Lenzen et al., 1996; Lenzen, 2008).

Pancreatic and duodenal homeobox 1 (Pdx-1) is a central transcription factor regulating pancreatic development and islet β cell function and maintaining β cell-specific gene expression (Kaneto et al., 2007). Constitutively overexpressed Pdx-1 also sensitizes β cells to cytokine-induced apoptosis (Ammendrup et al., 2000; Nielsen et al., 1999, 2004). However, the molecular mechanisms of Pdx-1-enhanced cytokine sensitivity need to be defined, since they represent potential therapeutic targets.

Cytokine exposure and subsequent NFκB activity are implicated in the metabolic syndrome leading to insulin resistance via both central and peripheral pathways (Arkan et al., 2005; Yuan et al., 2001; Cai et al., 2005; Zhang et al., 2008). Likewise, cytokine-mediated β cell apoptosis depends on persistent activation of the MAP kinase and NFκB signaling pathways (Aikin et al., 2004; Eldor et al., 2006; Giannoukakis et al., 2000;

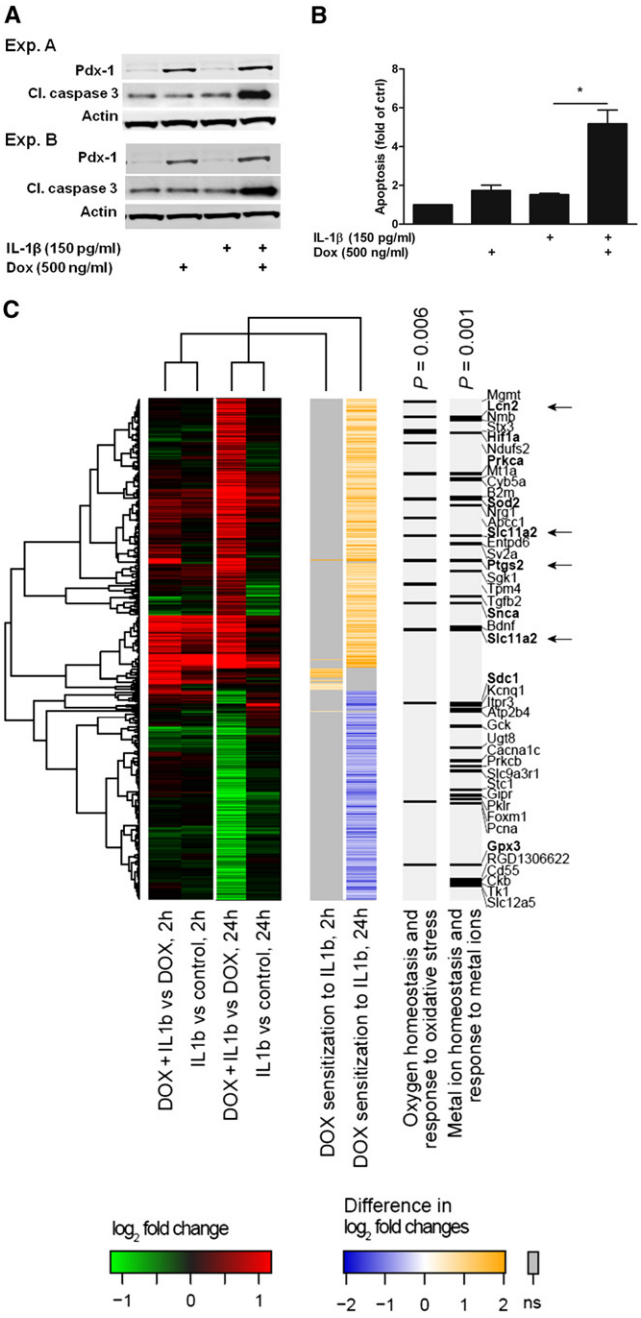

Figure 1. Pdx-1 Overexpression Sensitizes β Cells to IL-1β-Induced Apoptosis and Induces Changes in Iron- and ROS-Related Gene Expression

(A) Replicate western blot analyses of cleaved caspase-3 after 24 hr of IL-1β exposure in INS-1rαβ cells with doxycycline (dox)-induced overexpression of Pdx-1.

(B) Apoptosis measured by cytosolic histone-DNA complexes in Pdx-1-overexpressing cells exposed to IL-1β for 24 hr. Graphs show means + SEM, n = 3–5, *p < 0.05, Student's t test.

(C) Left: Heat map showing log2-transformed fold changes of genes in INS-1rαβ cells with or without Pdx-1 overexpression upon 2 and 24 hr exposure to 150 pg/ml IL-1β (IL1b). Rows represent the 693 individual probe sets. Middle: Log2-transformed gene changes after IL-1β exposure in INS-1rαβ cells with or without Pdx-1 overexpression upon 2 and 24 hr exposure to IL-1β. Right: Positions (black bars) of genes involved in ROS and iron related biological processes. Genes marked in bold are involved in both processes of which three were NFκB targets (arrows). Slc11a2 appeared twice in the microarray, representing DMT1 with the +IRE and DMT1 with both the +IRE and –IRE isoforms. p values were calculated by hypergeometric testing.

See also Figure S1.

Heimberg et al., 2001; Ortis et al., 2006). The molecular mechanisms involve endoplasmic reticulum stress, mitochondrial dysfunction, and ROS generation (Donath et al., 2008). ROS potentiates NFκB transcriptional activity, thereby establishing a vicious cycle of progressive cellular imbalance between pro- and antioxidant factors, leading to oxidative stress and cell damage (Lenzen et al., 1996; Lenzen, 2008; Tiedge et al., 1997).

Here, we hypothesized that β cells may be primed to inflammatory damage not only because of inadequate antioxidative defense but also due to aberrantly increased ROS production associated with cytokine-induced Pdx-1-dependent upregulation of proteins controlling cellular iron import.

RESULTS

Pdx-1 Overexpression Sensitizes to IL-1β-Induced Apoptosis

Pdx-1-overexpressing cells (Wang et al., 2001; Wang et al., 2005) (Figures S1A and S1B available online) were more sensitive to the proapoptotic action of IL-1β, as demonstrated by cleavage of caspase-3 and cytoplasmic histone-DNA complexes, when compared to cells not exposed to dox- or dn-Pdx-1-overexpressing cells (Figures 1A, 1B, S1C, and S1D). IL-1β or IL-1β plus IFN-γ-induced cleaved caspase-3 was also significantly enhanced in insulin-positive compared to insulin-negative primary rat acinar and human fetal liver cells transdifferentiating into β cell phenotypes (Baeyens et al., 2005; Zalzman et al., 2003; Zalzman et al., 2005) (Figures S1E and S1F).

To elucidate mechanisms of action underlying Pdx-1-driven potentiation of β cell sensitivity to IL-1β, we performed a microarray analysis of INS-1αβ cells with and without Pdx-1 overexpression exposed to 150 pg/ml IL-1β for 2 and 24 hr. A three-step bioinformatic procedure was applied to identify differentially expressed genes in response to IL-1β, depending on the presence or absence of Pdx-1 overexpression. First, we confirmed time-dependent regulation of numerous gene clusters by IL-1β by recording the differences between control INS-1rαβ versus IL-1β exposed INS-1rαβ cells not overexpressing Pdx-1 (Figure 1C, left). Second, gene expression in INS-1rαβ cells overexpressing Pdx-1 in the presence or absence of IL-1β differed with regard to 693 probe sets (Figure 1C, middle). Third, among the Pdx-1-dependent IL-1β-responding genes identified in this manner, enrichment analysis highlighted significant overrepresentation of genes implicated in oxygen homeostasis and response to oxidative stress (Figure 1C, right, lane 1, p = 0.006) and metal ion homeostasis and response to metal ions (Figure 1C, right, lane 2, p = 0.001), respectively.

Nineteen transcription factors (TFs) significantly regulating Pdx-1-dependent differential gene expression in IL-1β-exposed INS-1rαβ cells were identified (Figure 2A). Using the STRING database (Szklarczyk et al., 2011), 16 of these 19 TFs demonstrated high-confidence interactions, with NFκB as a central

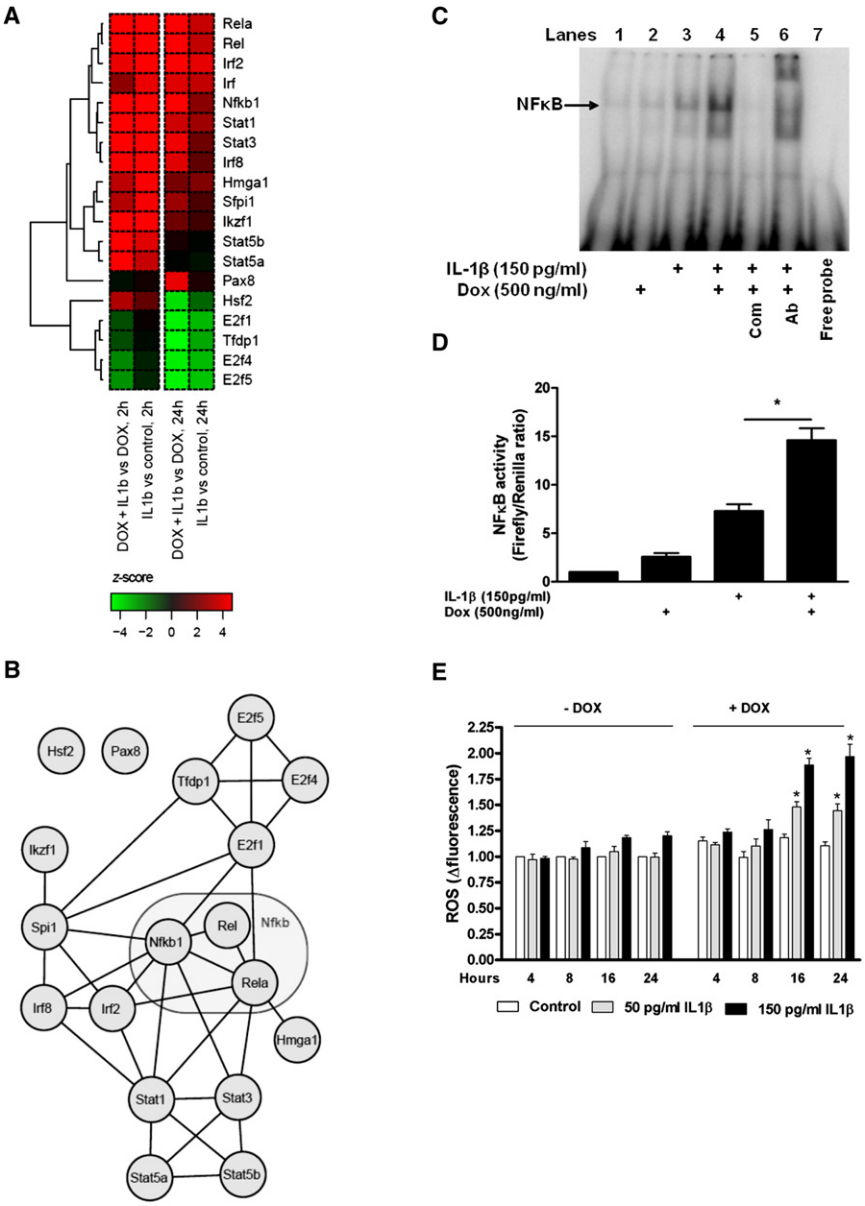

Figure 2. IL-1β-Induced NFκB Signaling Is Increased in Pdx-1-Overexpressing Cells

(A) Heat map showing *Z* scores for transcription factor genes with significantly induced (red) or repressed (green) expression upon exposure to 150 pg/ml IL-1β for 2 and 24 hr.

(B) Network of the 16 transcription factors with high-confidence associations.

(C) Nuclear extracts from Pdx-1-overexpressing INS-1rαβ cells exposed to IL-1β (150 pg/ml) for 1 hr. Nuclear extracts were subjected to electrophoretic mobility shift assay (EMSA) with a radioactively labeled NFκB-binding oligonucleotide as probe. Lane 1, control cells; lane 2, Pdx-1-overexpressing cells; lane 3, IL-1β-exposed cells; lane 4, Pdx-1-overexpressing and IL-1β-exposed cells; lane 5, competition (Com) with excess (×100) cold probe; lane 6, supershift with p65 antibody (Ab); lane 7, free probe. The EMSA is representative of n = 2.

(D) Cells were transiently transfected with an NFκB Firefly Luciferase construct in addition to a Renilla Luciferase construct as internal control. Cells were then treated with doxycycline (dox) for 24 hr followed by 6 hr exposure to 150 pg/ml IL-1β. Means + SEM, n = 6, *p < 0.05, Student's t test.

(E) IL-1β-induced reactive oxygen species (ROS) production in INS-1rαβ ± Pdx-1 overexpression was measured with a fluorescent, cell-permeable indicator for reactive oxygen species (CM-H2DCFDA). Means + SEM of n = 3, *p < 0.05, Student's t test.

See also Figure S2.

signaling node and direct associations to seven of these 16 TFs (Figure 2B). When linking the Pdx-1-dependent differentially regulated genes in Figure 1C with the TF analysis in Figures 2A and 2B, NFκB target genes associated with oxygen homeostasis and response to oxidative stress, as well as with iron homeostasis and response to metal ions, were overrepresented (genes in bold, Figure 1C). Three NFκB targets, *Slc11a2* (*solute carrier family 11, member 2* also named *iron transporting divalent metal transporter 1* [*Dmt1*]), *lipocalin 2* (*Lcn2*), and *prostaglandinendoperoxide synthase/cyclooxygenase* (*Ptgs2*), were significantly overrepresented in both the oxygen homeostasis and response to oxidative stress, as well as the iron homeostasis and response to metal ions pathways (p = 0.005). We therefore progressed with experimental validation of the roles of NFκB, DMT1, iron transport, and ROS in sensitizing β cells to inflammatory damage.

Pdx-1 Expression Facilitates IL-1β Induced NFκB Activity and ROS Formation

IL-1β exposure causes a rapid and sustained proapoptotic activation of NFκB and MAPK in β cells (Ammendrup et al., 2000; Eldor et al., 2006; Giannoukakis et al., 2000; Heimberg et al., 2001; Larsen et al., 1998; Ortis et al., 2006). Since the transcription factor network in Figure 2B indicated a central role for NFκB activity in Pdx-1 sensitization of β cells to IL-1β toxicity, we investigated the effect of Pdx-1 overexpression on IL-1β-induced NFκB activation. IL-1β-induced NFκB activity was increased in Pdx-1-overexpressing cells compared to wild-type and dn-Pdx-1-overexpressing cells, measured by increased IκBα degradation, binding of p65 to oligonucleotide κB binding sites, and NFκB transcriptional activity (Figures 2C, 2D, S2A, S2C, and S2D). Accordingly, we found increased expression of several NFκB target genes in Pdx-1-overexpressing cells compared to wild-type cells (Figure S2B).

The microarray analysis highlighting regulation of genes implicated in oxygen homeostasis and responses to oxidative stress was validated by the finding that IL-1β-induced ROS formation was significantly enhanced in the INS-1rαβ cells overexpressing Pdx-1 (Figure 2E).

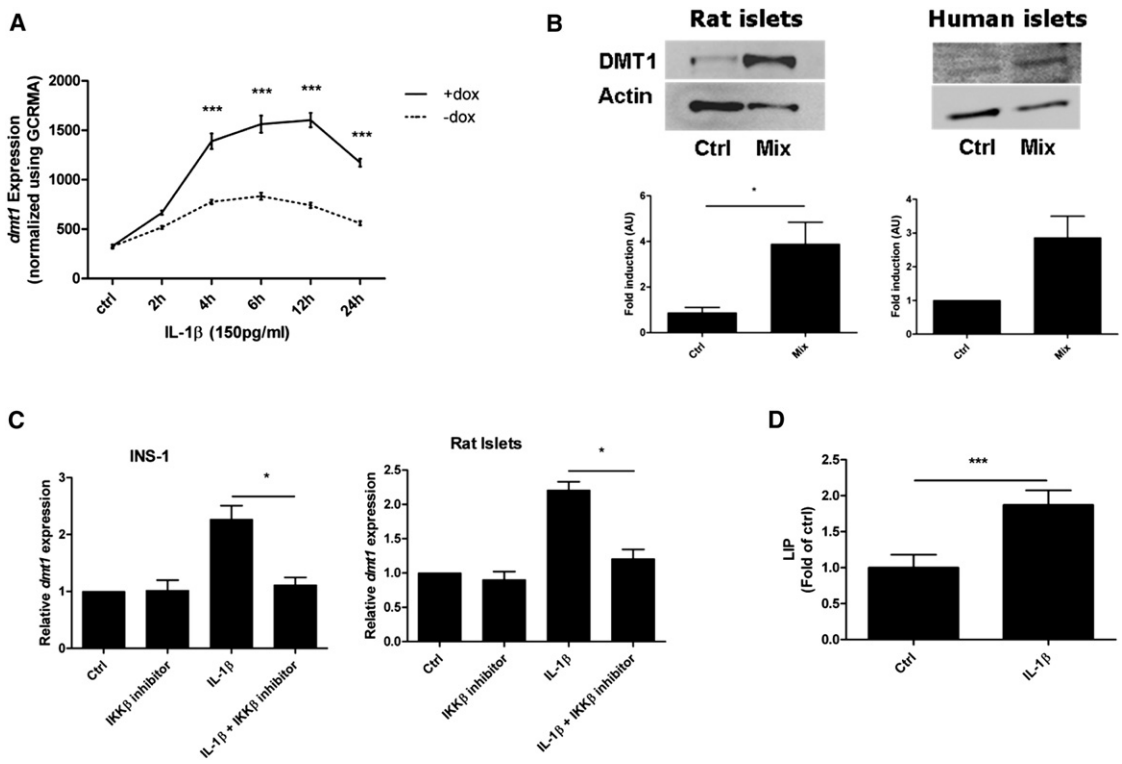

Figure 3. IL-1β Exposure Increases Expression of the Iron Transporter DMT1 in β Cells

(A) Quantification of mRNA from the microarray in Figure 1C showing 150 pg/ml IL-1β-induced DMT1 expression in INS-1rαβ with or without Pdx-1 overexpression induced by doxycycline (dox). Means + SEM of four individual experiments, ***$p < 0.001$, two-way ANOVA.

(B) Western blot analysis for DMT1 in lysates of rat islets (left) exposed to 150 pg/ml IL-1β + 5 ng/ml IFN-γ (Mix) for 24 hr. Blot is representative of n = 5. Quantification of DMT1 protein expression in islets from two human donors (right) exposed to 160 pg/ml IL-1β + 5 ng/ml IFN-γ (Mix) for 10 hr. Graphs show means + SEM.

(C) DMT1 gene expression determined by real-time qPCR of IL-1β-exposed INS-1 cells (left) or rat islets (right) precultured with a cell-permeable IKKβ inhibitor (1 μM). The graph shows means + SEM, n = 3, *$p < 0.05$, Student's t test.

(D) Effect of a 24 hr IL-1β exposure of isolated rat islets on the intracellular labile iron pool (LIP), measured as quenching of calcein fluorescence. Means + SEM, n = 4, paired Student's t test, ***$p < 0,005$.

See also Figure S3.

IL-1β Induces Islet Expression of the Iron Transporter DMT1

Having demonstrated that Pdx-1 facilitates IL-1β signaling we focused on the expressional regulation of the NFκB-regulated iron transporter DMT-1 (Ingrassia et al., 2012; Paradkar and Roth, 2006a). IL-1β-induced DMT1 messenger RNA (mRNA) expression as found by microarray comparison of INS-1rαβ cells with and without Pdx-1 overexpression was verified by western blotting showing increased DMT1 protein expression in cytokine-exposed rat islets and islets from two human donors (Figures 3A and 3B).

The gene cluster analysis in Figure 2B pointed to NFκB as central signaling node in the network, and the DMT1 promoter contains NFκB binding sites (Paradkar and Roth, 2006a, 2006b). We therefore pre-exposed INS-1 cells and isolated rat islets to a cell-permeable IKKβ inhibitor that blocks NFκB activation (Figure S3A) (Friberg et al., 2010). IKKβ inhibition almost completely prevented IL-1β-induced *Dmt1* mRNA expression, demonstrating pronounced dependence of IL-1β-induced *Dmt1* expression on NFκB activity (Figure 3C).

IL-1β Increases Islet Labile Iron Pool

Using confocal microscopy, we localized DMT1 to islet cell cytosol, with a staining pattern compatible with endosomal compartmentalization (Figure S3B). Since DMT1 is a transmembrane iron transporter involved in endosomal-to-cytoplasmic iron transport (Mims and Prchal, 2005), we next showed that IL-1β-induced increase in DMT1 expression correlated with increased intracellular labile iron pool (LIP) in rat islets (Figure 3D). This correlated with increased expression of *Lcn2* and *transferrin receptor* (*TrfR*), known mediators of iron import, and decreased expression of the iron exporter *ferroportin* (Figure S3C). Thus, inflammatory conditions promote reprogramming of the β cell to favor iron accumulation.

Iron Chelation and DMT-1 siRNAs Protect against Cytokine-Induced β Cell Apoptosis

IL-1β-induced ROS formation and apoptosis were inhibited by the iron chelators desferrioxamine (DFO) and deferasirox (D-Sirox) in primary rat islets and in INS-1E cells, effects that were reversed by subsequent medium replenishment of iron

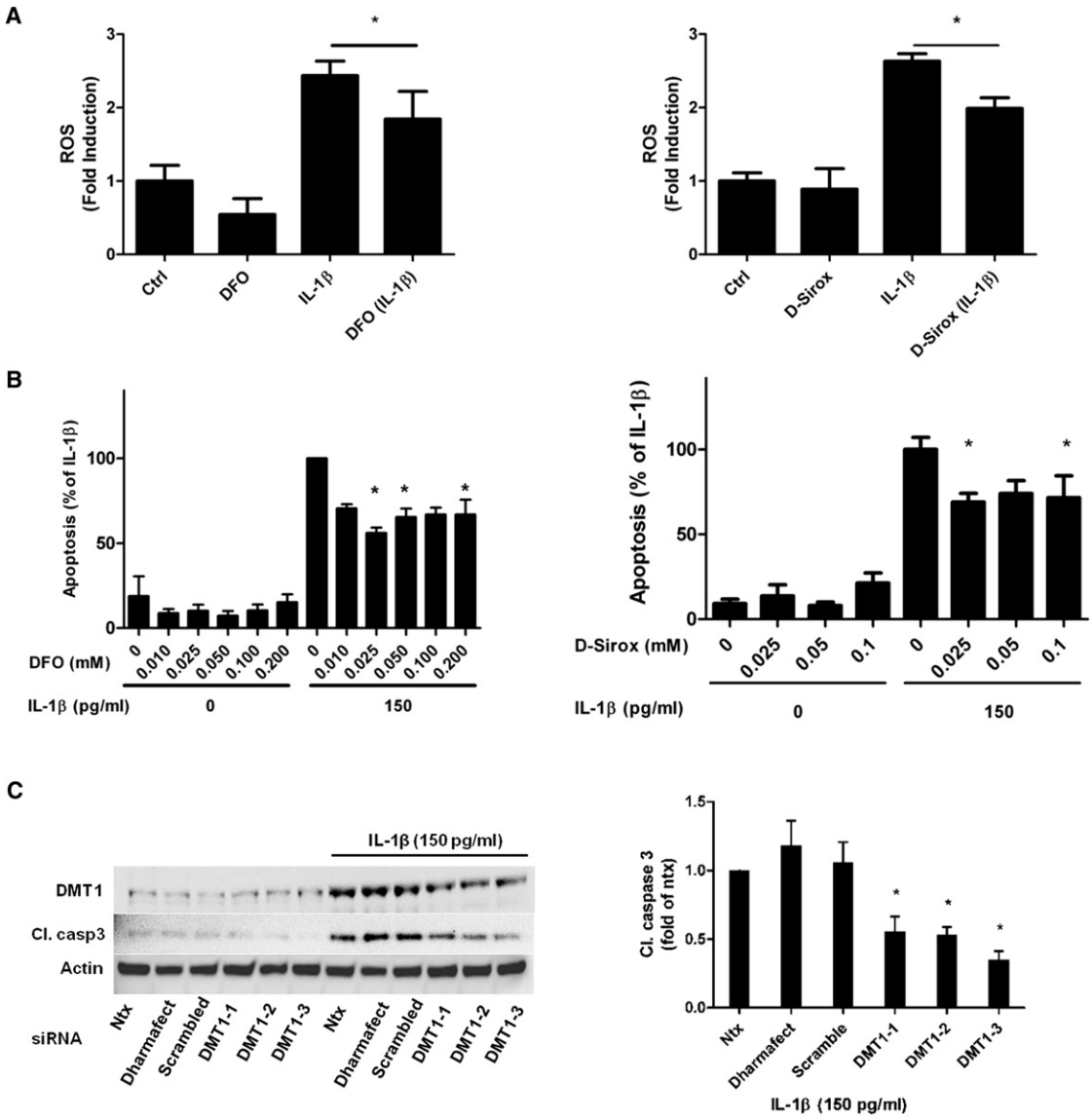

Figure 4. Iron Chelation and DMT1 Knockdown Protect against IL-1β-Induced ROS Formation and Apoptosis

(A) Inhibition of 150 pg/ml IL-1β-induced ROS formation in rat islets pretreated for 24 or 1 hr, respectively, with the iron chelators desferrioxamine (DFO) (0.1 mM) or deferasiox (D-Sirox) (0.025 mM). ROS was measured with the fluorescent, cell-permeable indicator CM-H2DCFDA. Means + SEM, n = 6, Student's t test, *p < 0.05.

(B) IL-1β-induced cell death measured as cytosolic DNA-histone complexes after 24 hr in rat islets pretreated with DFO or D-Sirox. Means + SEM, n = 3–4, *p < 0.05, Student's t test.

(C) INS-1 cells were left nontransfected (ntx), or transfected with 30 nM of control (Dharmafect), scrambled siRNA, or three different siRNA targeting DMT1. After 2 days of recovery, cells were left untreated or exposed to 150 pg/ml IL-1β for 24 hr. Western blotting of cell lysates with DMT1 and cleaved caspase-3 (cl. casp3)- and β-actin-specific antibodies was performed (left). Mean optical density measurements of cleaved caspase-3 were corrected for protein loading by β-actin in IL-1β-exposed cells (right). n = 6, means + SEM, *p < 0.05, Student's t test.

See also Figure S4.

(Figures 4A, 4B, S4A, and S4B). Additionally, DMT1 knockdown with three different DMT1-targeted small interfering RNAs (siRNAs) resulted in a reduction of IL-1β-induced DMT1 expression and cleaved caspase-3 in INS-1E cells (Figure 4C).

β Cell-Specific *Dmt1* Knockout Protects from Cytokine-Induced Apoptosis

We generated an inducible β cell-specific *Dmt1* knockout (KO) mouse by crossing a floxed *Dmt1* mouse (Gunshin et al., 2005), with a mouse carrying the *cre recombinase* (*cre*) gene fused to the mutated estrogen receptor driven by the Pdx-1 promoter (Gu et al., 2002), resulting in specific excision of exons 6–8 of the *Dmt1* gene in Pdx-1-expressing cells upon tamoxifen treatment (Figure 5A). In animals carrying the *cre* gene, cre translocation was observed in most insulin-positive cells 12 hr after tamoxifen treatment (Figure 5B). A *Dmt1* knockdown efficiency of approximately 80% as quantified by RT-PCR of mRNA from isolated islets was anticipated since islets contain

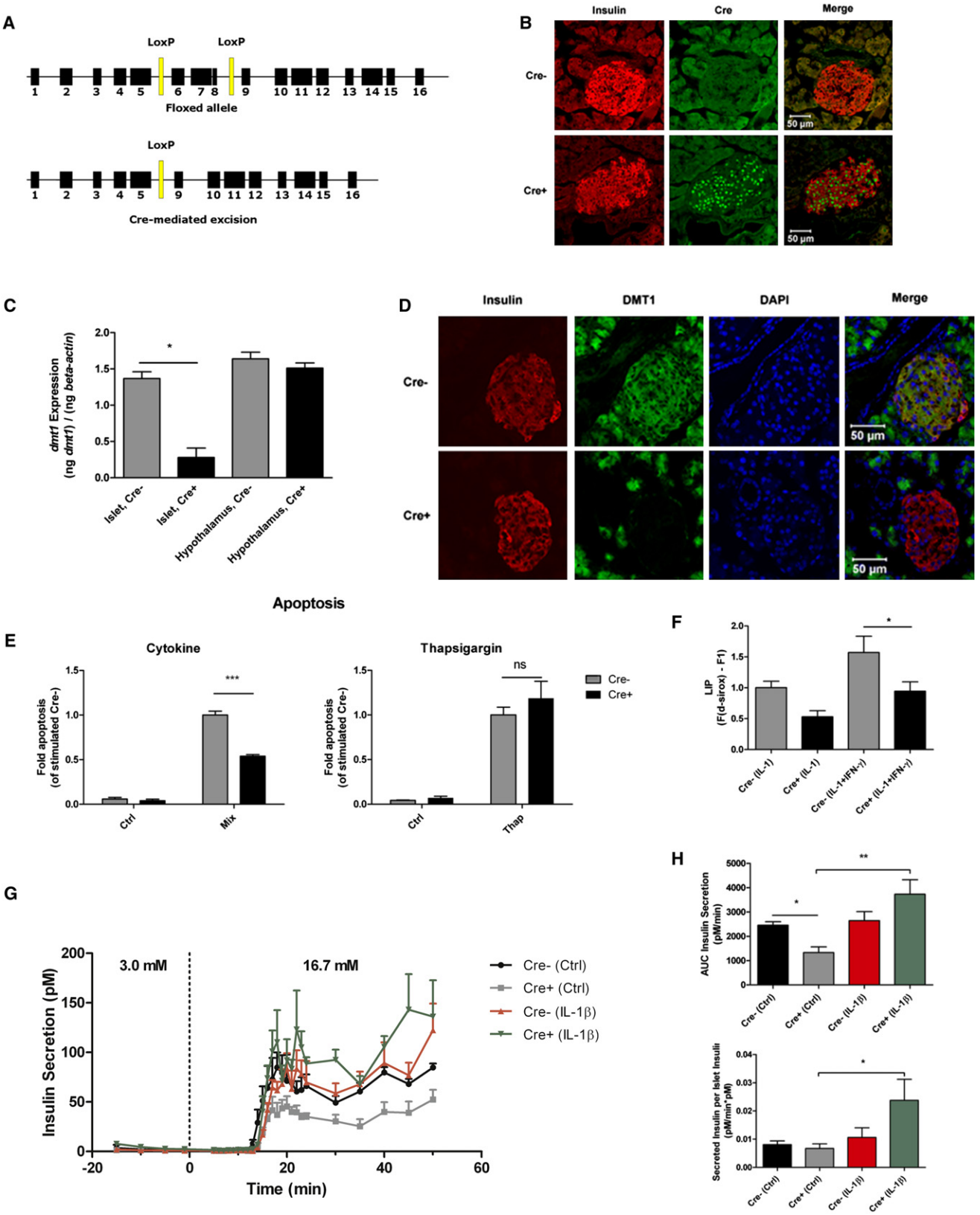

Figure 5. DMT1 Deletion Protects β Cells from Cytokine-Induced Apoptosis

(A) Tamoxifen (TAM)-inducible cre-lox recombination was used to generate β cell-specific DMT1 knockout mice. Exons 6–8 were excised by cre-mediated recombination.

approximately 70% β cells (Figure 5C). Since Pdx-1 driven cre recombinase activity using lacZ or X-gal reporters has been shown in hypothalamic neurons (Wicksteed et al., 2010), we showed that total hypothalamic *Dmt1* expression was cre recombinase insensitive (Figure 5C); however, this finding does not exclude that *Dmt1* expression in hypothalamic subregions is cre recombinase sensitive or that central-peripheral pathways may impact β cell function in the *Dmt1* knockout mouse. DMT1 is highly expressed in both the exocrine and endocrine pancreas in WT mice; tamoxifen treatment caused complete and β cell-specific knockout of DMT-1 in islets from the *Cre*+ mice without compensatory changes in other iron transport-regulating genes (Figures 5D and S5A). *Dmt1* KO did not induce ultrastructural changes in β cells (Figure S5B). Cytokine-induced apoptosis in islets from *Dmt1* KO mice was reduced by approximately 45% compared to WT islets (Figure 5E, left), consistent with the levels of protection obtained by iron chelation and siRNA knockdown of DMT-1 in vitro (Figure 4). *Dmt1* knockout did not protect against apoptosis induced by thapsigargin, a potent inducer of ROS- and cytokine-independent islet cell apoptosis mediated via inhibition of smooth endoplasmic reticulum calcium ATPase 2B (Tonnesen et al., 2009) (Figure 5E, right). LIP was significantly reduced in IL-1β and IFN-γ exposed *Dmt1* knockout islets (Figure 5F).

Dmt1 Knockout Improves Glucose-Stimulated Insulin Secretion and Insulin Secretory Efficacy in IL-1β-Exposed Islets

The stimulus-secretion coupling in insulin exocytosis involves a glucose oxidation-dependent increase in the ATP/ADP ratio but also ROS generation (Leloup et al., 2009). We therefore anticipated that first-phase glucose-stimulated insulin secretion (GSIS) would be lower in *Dmt1* KO islets unchallenged by inflammatory assault ex vivo. Indeed, this was the case (Figures 5G and 5H, top), highlighting a physiological role of iron and ROS in the regulation of insulin exocytosis. Second-phase GSIS was also significantly reduced, showing that glucose-induced insulin synthesis is also iron dependent. In contrast, when exposed to IL-1β, both first- and second-phase GSIS from *Dmt1* KO islets were significantly higher compared both to cytokine-exposed *cre*– islets and control *cre*+ islets (Figures 5G and 5H, top). Insulin secretory efficacy expressed as a ratio between the area under the curve of secreted insulin during the first and second phase and the islet insulin content at the end of the perifusion was unaffected in cytokine-nonexposed *Dmt1* KO islets ex vivo but markedly higher in these islets after exposure to IL-1β (Figure 5H, bottom, and Figure S5C).

Dmt1 KO Improves Glucose Tolerance and Circulating Insulin Levels in Multiple Low-Dose Streptozotocin and High-Fat Diet-Induced Diabetes, Models of Type 1 and Type 2 Diabetes, Respectively

To test the relevance of our model in type 1 and type 2 diabetes, we characterized the metabolic phenotypes of (1) mice receiving multiple low-doses of streptozotocin (MLDS) to provoke immune-mediated β cell destruction and diabetes, (2) mice fed a high-fat diet (HFD), and (3) unchallenged mice (Figures 6 and S6).

In the MLDS model of type 1 diabetes (Leiter, 1982), β cell destruction in *cre*– mice was evidenced by a significant increase in fasting blood glucose levels at day 19, 11 days after the last injection of streptozotocin (Figures 6A and 6B) but MLDS had no effect on weight and body composition (Figures 6C and S6A). From day 19 to the end of the experiment on day 99, the area under the fasting glucose curve was significantly reduced, and glucose tolerance and circulating insulin levels were significantly improved in MLDS treated *Dmt1* KO mice (Figures 6B and 6D–6F).

HFD-induced diabetes in rodents leading to low-grade islet inflammation and progressive β cell dysfunction and apoptosis is a model of human type 2 diabetes (Eguchi et al., 2012; Ehses et al., 2007). HFD significantly increased body weight and fat body mass and reduced lean body mass in both *cre*– and *cre*+ animals (Figures 6G and S6B). No effect of β cell-specific *Dmt1* KO on body composition was observed (Figures 6G and S6B). In HFD *Dmt1* KO mice, glucose tolerance was significantly improved, correlating with significantly enhanced insulin secretion in these animals (Figures 6H–6J).

The early effects of DMT1 deletion on β cell function were investigated by glucose tolerance testing of unchallenged mice. Three weeks after tamoxifen treatment, *cre*– and *cre*+ animals had normal glucose tolerance and insulin sensitivity suggesting that the secretory defect demonstrated in unchallenged β cell-specific *Dmt1* KO ex vivo was compensated in vivo (Figure S6C). Intermediate and long-term *Dmt1* deletion studied 5 and 21 weeks after tamoxifen treatment had no effects on β cell function in the control groups from the MLDS and HFD protocols, respectively (Figures 6D–6F and 6H–6J).

(B) Immunohistochemical analysis of pancreata from TAM-treated mice was performed to verify nuclear cre translocation 12 hr after the last TAM injection.
(C) DMT1 gene expression in isolated islets and hypothalamus from *cre*− and *cre*+ mice by RT-PCR (n = 3–5, +SEM, *p < 0.05, Student's t test).
(D) Verification of DMT1 KO by immunohistochemistry of pancreatic sections 2 weeks after completed TAM treatment.
(E) Left: Cytokine induced apoptosis in isolated islets from TAM treated *cre*− and *cre*+ animals measured as cytosolic DNA-histone complexes after 16 hr of exposure to a mixture of 300 pg/ml IL-1β and 10 ng/ml IFN-γ (Mix) (right), n = 4, +SEM, ***p < 0.001 with two-way ANOVA. Right: Thapsigargin- (10 μM) induced apoptosis in isolated islets from TAM treated *cre*− and *cre*+ animals measured as cytosolic DNA-histone complexes after 24 hr, n = 4, means + SEM. ns, not significant.
(F) Determination of the labile iron pool (LIP) in IL-1β- and IL-1β+IFN-γ-exposed islets isolated from cre– and cre+ mice. Means + SEM of n = 3–6, Student's t test, *p < 0.05.
(G) Insulin secretion from isolated *cre*− and *cre*+ islets was measured after perifusion. Control or IL-1β-exposed islets were perifused with Krebs Ringer's solution supplemented with 3.0 mM glucose for 30 min, and then with 16.7 mM glucose for 50 min. Means + SEM of five independent experiments are shown.
(H) Top: Area under the curve from perifusion experiment. Bottom: Total islet insulin was extracted after perifusion, and islet secretory efficacy was calculated as the area under the curve over islet insulin content ratio. Graphs show means + SEM, n = 5.
See also Figure S5.

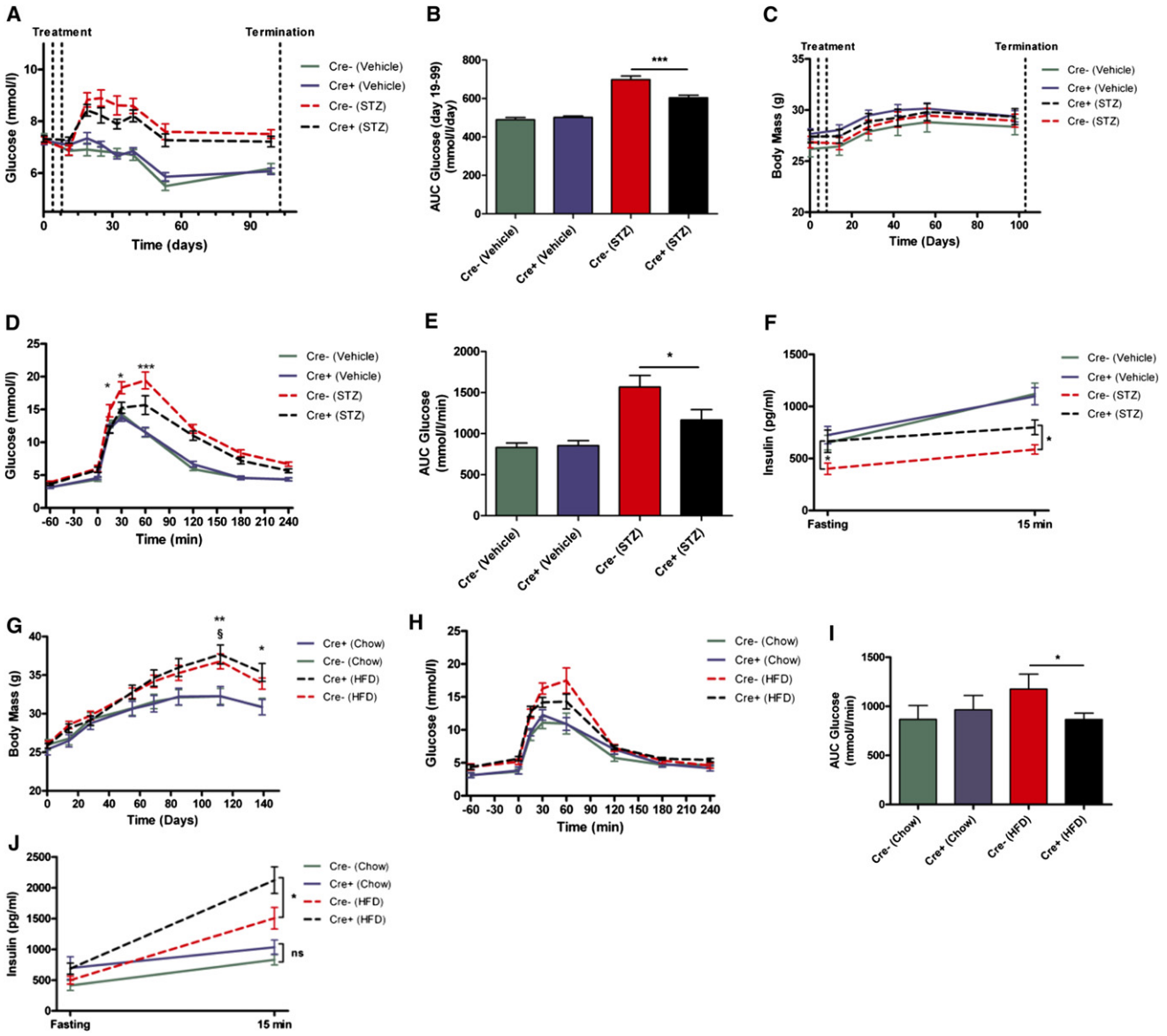

Figure 6. β Cell-Specific DMT1 Knockout Lowers Blood Glucose and Improves Glucose Tolerance in Mice Treated with Multiple Low-Dose Streptozotocin and High-Fat Diet

(A) Blood glucose in 4 hr fasted *cre*− and *cre*+ mice treated with vehicle or streptozotocin (STZ) for the period indicated (Treatment). The graph shows means + SEM, n = 16–18.

(B) Area under the curve of blood glucose from day 19 to 99. Means + SEM, n = 16–18, ***p < 0.001, Student's t test.

(C) Weight development in STZ- and vehicle-treated DMT1 KO and WT mice. Means + SEM, n = 16–18.

(D) Oral glucose tolerance test (OGTT) in STZ-treated DMT1 KO and WT mice. Mice were fasted overnight and were given an oral gavage of 2.0 g/kg glucose at 0 min. Means + SEM, n = 16–18, *p < 0.05, ***p < 0.001, two-way ANOVA with repeated measures and Bonferroni's post-hoc test.

(E) Area under the curve of OGTT. Means + SEM, n = 16–18, Student's t test.

(F) Fasting and OGTT-induced insulin secretion. Samples were taken 60 min before and 15 min after oral gavage. Means + SEM, n = 16–18, *p < 0.05, Student's t test.

(G) Weight development in HFD and chow-fed DMT1 KO and WT mice. Means + SEM, n = 10–15, §p < 0.05 *cre*− (HFD) versus *cre*− (chow), *p < 0.05 **p < 0.01 *cre*+ (HFD) versus *cre*+ (chow).

(H) OGTT in DMT1 KO and WT mice after 21 weeks of high-fat feeding. Means + SEM, n = 10–15.

(I) Area under the curve of OGTT in HFD DMT1 KO and WT mice. Means + SEM, n = 10–15, *p < 0.05, Student's t test.

(J) Fasting and OGTT-induced insulin secretion. Samples were taken 60 min before and 15 min after oral gavage. Means + SEM, n = 10–15, *p < 0.05, Student's t test.

See also Figure S6.

DISCUSSION

Our data suggest that aberrant cytokine-dependent upregulation of cellular iron import via DMT1 primes β cells to ROS-mediated inflammatory damage in a Pdx-1 dependent manner (Figure 7) by enhancing NFκB transcriptional activity, either by central or peripheral pathways or both.

Pdx-1 has been suggested to recruit histone deacetylases (HDAC) 1 and 2 to the insulin promoter (Mosley and Ozcan, 2004). We recently found that small-molecule HDAC inhibitors reduce cytokine-induced NFκB transcriptional activity and apoptosis in insulin-producing cells by inhibiting p65 DNA binding (Christensen et al., 2011), and we confirmed this by HDAC1 siRNA (Lundh et al., 2012). Accordingly, we hypothesize that Pdx-1 may also recruit HDAC1 to the *Dmt1* promoter, thereby facilitating p65 binding and DMT1 gene transcription, although a canonical Pdx-1 *cis*-binding element has yet to be determined in the DMT1 promoter.

In vitro, β cell iron depletion with two different iron chelators and DMT1 deletion by both siRNA and transgenic approaches significantly decreased IL-1β-induced ROS production and β cell apoptosis. In vivo, *Dmt1* KO improved glucose tolerance and circulating insulin levels in multiple low-dose streptozotocin and high-fat diet-induced diabetes, models of islet inflammation in type 1 and type 2 diabetes, respectively. These data provide a molecular link explaining why iron chelator treatment improved glucose tolerance and insulin secretion in the genetically obese and diabetic ob/ob mouse (Cooksey et al., 2010) and why feeding the OLETF rat model of obesity and diabetes an iron-restricted diet increased plasma insulin levels and pancreatic insulin content (Minamiyama et al., 2010).

The partial protection against IL-1β-induced β cell toxicity conferred by iron chelation or *Dmt1* knockdown was remarkably consistent across our experimental models, emphasizing the validity of the concept. Of note, Pdx-1-mediated sensitization to IL-1β-induced apoptosis correlated also with enhanced JNK, but not p38 or ERK MAPK activation, and inhibition of JNK activity is known to reduce cytokine-mediated β cell damage (Ammendrup et al., 2000; Bonny et al., 1998). Whether JNK activation is secondary to DMT1-facilitated ROS formation, or other priming pathways controlled by Pdx-1, remains to be shown. However, when taken together, these observations underscore that DMT1-dependent iron transport and ROS formation is not an exhaustive explanation for Pdx-1-mediated sensitization to inflammatory β cell damage, but that several mechanisms yet to be demonstrated may operate in parallel.

Total hypothalamic DMT1 expression was cre recombinase insensitive in our *Dmt1 null* mice. Notably, this finding does not exclude that DMT-1 expression in hypothalamic subregions is cre recombinase sensitive, and that central-peripheral pathways may impact β cell function in the *Dmt1 null* mouse. Indeed, inflammatory activation of the IKK/NFκB pathway in the liver and hypothalamus are important in the pathogenesis of type 2 diabetes (Cai et al., 2005; Zhang et al., 2008; De Souza et al., 2005; Milanski et al., 2012; Moraes et al., 2009).

Tissue targets of iron-driven cellular insults such as hepatocytes, cardiomyocytes, and pancreatic β cells typically have high mitochondrial activity. Hence, cirrhosis and hepatomas, heart failure, and diabetes are well-known complications to iron overload conditions (Aldouri et al., 1990; Eaton and Qian, 2002; Gabutti and Borgna-Pignatti, 1994; Niederau et al., 1985; Rajpathak et al., 2009). It is likely that this association involves a toxic effect of iron-catalyzed ROS on cellular organelles, in particular highly active mitochondria and lysosomes (Eaton and Qian, 2002). This is supported by findings of oxidative stress-induced decreased insulin secretory capacity and β cell apoptosis in mouse models of primary hemochromatosis (Cooksey et al., 2004), and reduced insulin secretion in patients with diabetes secondary to hemochromatosis (McClain et al., 2006), in whom the insulin secretory defect can be ameliorated by correcting iron overload by phlebotomy (Abraham et al., 2006).

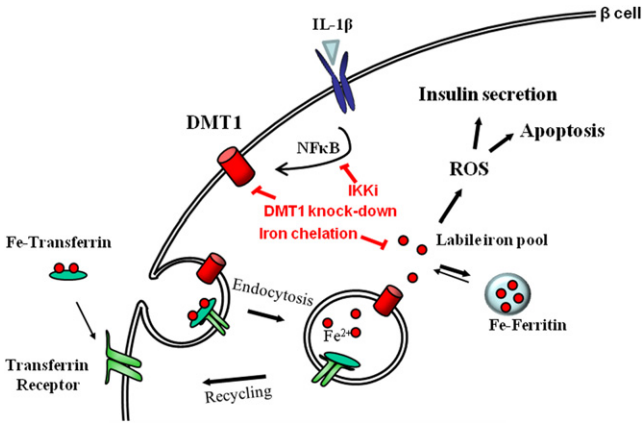

Figure 7. Schematic Illustration of IL-1β-Induced Iron Uptake, ROS Production, and Apoptosis in β Cells

In Pdx-1-expressing cells, binding of IL-1β to the receptor complex initiates a cascade of NFκB-dependent DMT-1 expression, iron uptake, and consequent iron-catalyzed ROS formation controlling β cell insulin secretion and apoptosis. This chain of events can be modified by inhibition of NFκB activation (IKKi), DMT knockdown (siRNA)/knockout (cre-lox), and iron chelation.

Our findings position DMT1 as an important interface between iron and immunity, and there is both preclinical and clinical data to support this notion. Intracellular iron accumulation mediates IFN-γ-, lipopolysacharide- (LPS), and TNF-α-induced oxidative stress and cell death in endothelial cells, hepatocytes, and the CNS (Autelli et al., 2005; Li and Frei, 2009; Nanami et al., 2005; Warren et al., 1993; Zhang et al., 2005). DMT1 is strongly expressed in human monocytes and synovial fibroblasts from patients with sterile inflammatory conditions such as rheumatoid arthritis, and IL-1β mediates increased iron uptake in these cell types (Telfer and Brock, 2002, 2004). Furthermore, the association between the increased expression of proinflammatory cytokines, pathological iron deposition, and oxidative stress in neurodegenerative disorders like Alzheimer's disease, Parkinson's disease, and multiple sclerosis points to cytokines and iron as central pathogenetic elements in the inflammatory processes leading to these conditions (Berg and Youdim, 2006; Du et al., 2009; Salazar et al., 2008; Zhang et al., 2005).

Novel orally effective and well-tolerated iron chelators have been developed and are now in routine clinical use for iron-overload related diseases (Cappellini and Piga, 2008). Iron chelation protects immune cells against oxidative stress-induced DNA

damage and cell death (Kurz et al., 2006; Persson et al., 2003; Yu et al., 2003), emphasizing the importance of endosomal/lysosomal redox-active iron in these processes. Iron chelation further protects and improves the function of islet grafts in animal models (Bradley et al., 1986; Nomikos et al., 1986; Vaithilingam et al., 2010), in line with our demonstration of desferrioxamine and deferasirox-mediated protection against cytokine-induced β cell apoptosis. Hence, our findings have translational relevance. Since large, prospective, epidemiological studies have shown that elevated transferrin saturation in the general population confers increased risk of developing any form of diabetes (Ellervik et al., 2011), careful iron chelator titration in individuals at risk of developing diabetes or even public health initiatives to lower iron saturation without causing anemia could be envisaged as measures to prevent diabetes development.

In summary, aberrant cytokine-dependent upregulation of cellular iron import via DMT-1 primes β cells to ROS-mediated inflammatory damage. This concept may be generalizable to other tissues that are targets of iron-overload damage and may open avenues for the development of novel therapies for chronic inflammatory diseases.

EXPERIMENTAL PROCEDURES

Details on reagents, cell lines, islet isolation, cell death, microarray, RT-PCR, immunoblotting, transient transfection and Luciferase assay, and immunohistochemistry are given in the Supplemental Experimental Procedures.

Islet Isolation

Pancreata were digested with collagenase, isolated by hand picking or gradient centrifugation, and cultured as described in the Supplemental Experimental Procedures.

Human Islets

Human islets were isolated from brain-dead donors with normal β cell function as described (Lehmann et al., 2004) in compliance with institutional ethical regulations and cultured as described (Maedler et al., 2004) with or without 160 pg/ml IL-1β plus 5 ng/ml IFN-γ for 10 hr.

KO Mice and Animal Care

Transgenic mice and Wistar rats were bred at Taconic (Ry, Denmark). All animals were maintained in a 12 hr light/dark cycle and fed ad libitum. The floxed *Slc11a2* mouse was generated previously (Gunshin et al., 2005). Floxed mice were crossed with a mouse carrying the *Cre-ERT* gene under control of the *Pdx-1* promoter from Dr. Melton's laboratory provided by Dr. Serup, the Hagedorn Research Institute, Gentofte, Denmark, and kept on a mixed background (Gu et al., 2002). *Cre−* and *cre+* mice were administered four consecutive intraperitoneal injections with tamoxifen (2.5 mg per mouse) (Sigma-Aldrich, Denmark) diluted in ethanol-corn oil at 8–12 weeks of age. Streptozotocin (Sigma-Aldrich) was dissolved in 0.1 M sodium-citrate (Sigma-Aldrich) buffer with pH 4.5, and administered for five consecutive days in a dose of 35 mg per kg body weight (BW). The β cell destruction was followed by 4 hr fasting blood glucose measurements. High-fat diet supplemented with 500 mg iron per kg was purchased from Research Diets (New Brunswick, NJ, product # D11101701). All animal work was performed following the guidelines and legislation of the Danish Animal Experiment Inspectorate.

Oral Glucose Tolerance Test and Plasma Insulin Measures

Mice were fasted over night (16 hr) and given an oral gavage of 2.0 g per kg BW of glucose (Sigma-Aldrich) diluted in water. For blood glucose measurements, tail vein blood was drawn, and blood glucose was measured with a hand-held Bayer glucometer (Leverkusen, Germany). Plasma was collected from eye blood for insulin determination in duplicates with a MesoScale Insulin Kit (Gaithersburg, MD).

Measurement of Cell Death

Apoptotic cell death was determined in duplicates of size-matched islets by the detection of DNA-histone complexes present in the cytoplasmic fraction of cells using Cell Death Detection ELISA^{PLUS} (Roche, Basel, Switzerland) (for details, see the Supplemental Experimental Procedures).

Transmission Electron Microscopy

Isolated islets cultured in 3.0 mM glucose medium for 2 hr to establish baseline insulin secretion and were then transferred to medium containing 16.7 mM glucose for 15 min prior to fixation in 2% glutaraldehyde in a 0.05 M phosphate buffer (pH 7.2). Sections were stained with uranyl acetate and lead citrate and were subsequently examined with a Philips CM 100 TEM (Philips, Eindhoven, The Netherlands) operated at an accelerating voltage of 80 kV. Digital images were recorded with an OSIS Veleta digital slow scan 2k × 2k CCD camera and the ITEM software package.

Nuclear Extract Electrophoretic Mobility Shift Assay

Cells were cultured in 10 cm dishes to 80%–85% confluence. Nuclear extracts were isolated and electrophoretic mobility shift assay (EMSA) carried out as described (Larsen et al., 2007). We controlled for loading by determining the protein concentration in all nuclear extracts before addition of an identical volume and excess amount (20 fmol) of radiolabelled oligonucleotide probe: 5′-GTCAGCTTCAGAGGGACTTTCCGAGAGG-3′. The protein concentrations in the nuclear extracts were identical between the experimental conditions, thereby allowing dilution with the same volume of buffer to obtain an identical final protein concentration in all reaction mixtures (reaction volume 20 μl) and the application of the same amount of protein (5 μg) per lane on the EMSA gels. In supershift experiments, nuclear extracts were preincubated with anti-p65 antibody (sc-37; Santa Cruz) for 30 min at 4°C.

Measurement of Intracellular Labile Iron Pool and Iron Supplement

The iron sensitive fluorescent dye calcein (Molecular Probes, Cambridge, UK) was used to evaluate the effect of cytokines on the labile iron pool (LIP) in islets (Epsztejn et al., 1997). In brief, islets were incubated in Krebs Ringer buffer with 10 mM glucose, 20 mM HEPES (GIBCO, Denmark) without bicarbonate (pH 7.3) with 0.25 μM calcein probe for 1 hr. Excitation was measured at 488 nm and emission at 517 nm. After fluorescence detection, the total amount of loaded calcein was detected after chelation of intracellular iron with 0.05 mM deferasirox for 15 min.

Measurement of Intracellular ROS/RNS Generation

ROS was measured by incorporation of 5-(and-6)-chloromethyl-2′,7′-dichlorodihydrofluorescein (H2DCFDA) (Molecular Probes, Invitrogen, Denmark). Cells or islets were incubated in the dark with 10 μM H2DCFDA in PBS (for cells) or Krebs Ringer buffer with 7 mM glucose (pH 7.4). Increase in fluorescence at 45 to 90 min was measured on a NovoStar Microplate Reader (Ramcon, Denmark). Results are shown as delta fluorescence (t 90 min – t 45 min).

siRNA Transfection

Cells were cultured in antibiotic-free medium for 24 hr before transfection overnight with 30 nM siRNAs targeting DMT1 or with scrambled siRNA (QIAGEN). Three different target siRNAs and one scrambled siRNA were used. For transfection, siRNA and Dharmafect (Dharmacon, Chicago, IL) were diluted separately in Optimem medium (Invitrogen) and incubated at room temperature for 5 min. Lipid-siRNA complexes were allowed to form at room temperature for 20 min in 1 μl Dharmafect:150 nM Optimem. After overnight transfection, the medium was replaced by regular culture medium for cell recovery.

Islet Perifusion

The islet perifusion system was provided by Dr. Herbert Y. Gaisano, and has been previously described (Kwan et al., 2007). Islets from *cre+* or *cre–* littermates were exposed 24 hr after isolation to cytokines. Fifty islets per condition were preincubated in RPMI with 3 mM glucose prior to perifusion. Free-floating islets were perifused, with a flow-rate of 1 ml per minute using Gilson Minipuls 3 peristaltic pump (Gilson, Middleton, WI), and insulin sampling was performed over 1 min. Baseline insulin secretion was established after 30 min perifusion with 3 mM glucose Krebs Ringer solution (pH 7.4, 0.1% BSA, 0.1 mM HEPES), and glucose-stimulated insulin secretion was determined by perifusion of

islets with 16.7 mM glucose in Krebs Ringer solution for 50 min. After perifusion, islets were collected, counted, and subjected to ethanol-HCl insulin extraction and insulin measured by ELISA as described (Kekow et al., 1988).

Statistical Analysis

Data were analyzed with an unpaired t test assuming equal variances, or one- and two-way ANOVA with either Dunett's or Bonferroni's post-hoc test. Results are means + SEM. p values under 0.05 were considered significant, indicated with *, while p values of $p < 0.01$ and $p < 0.001$ are marked with ** and ***, respectively.

ACCESSION NUMBERS

The Gene Expression Omnibus (GEO) accession number for the microarray data reported in this paper is GSE40642.

SUPPLEMENTAL INFORMATION

Supplemental Information includes Supplemental Experimental Procedures and six figures and can be found with this article online at http://dx.doi.org/10.1016/j.cmet.2012.09.001.

ACKNOWLEDGMENTS

We would like to thank Dr. Claes Wollheim for providing the INS-1 cell lines, Drs. Doug Melton and Palle Serup for the *Cre-ERT* mouse line, Dr. Herbert Y. Gaisano for permission to apply his islet perifusion system, and Dr. Canonne-Hergaux for the anti-mouse DMT1 antibody. Louise Koch, Christine Petersen, Charity MK Graae, and Tine Wille are thanked for technical help with the DMT1 KO animals and in vitro assays. This work was supported by the JDRF Center for Beta Cell Therapy under the EU6FP, grant number LSHB-CT-2005-512145 (M.F.T.), a PhD fellowship from SHARE LIFE, Denmark (J.B.H.), UNIK: Food, Fitness & Pharma for Health and Disease (see www.foodfitnesspharma.ku.dk) supported by the Danish Ministry of Science, Technology and Innovation, and Novo Nordisk.

Received: June 9, 2011
Revised: June 27, 2012
Accepted: August 27, 2012
Published online: September 20, 2012

REFERENCES

Abraham, D., Rogers, J., Gault, P., Kushner, J.P., and McClain, D.A. (2006). Increased insulin secretory capacity but decreased insulin sensitivity after correction of iron overload by phlebotomy in hereditary haemochromatosis. Diabetologia *49*, 2546–2551.

Aikin, R., Maysinger, D., and Rosenberg, L. (2004). Cross-talk between phosphatidylinositol 3-kinase/AKT and c-jun NH2-terminal kinase mediates survival of isolated human islets. Endocrinology *145*, 4522–4531.

Aldouri, M.A., Wonke, B., Hoffbrand, A.V., Flynn, D.M., Ward, S.E., Agnew, J.E., and Hilson, A.J. (1990). High incidence of cardiomyopathy in beta-thalassaemia patients receiving regular transfusion and iron chelation: reversal by intensified chelation. Acta Haematol. *84*, 113–117.

Ammendrup, A., Maillard, A., Nielsen, K., Aabenhus Andersen, N., Serup, P., Dragsbaek Madsen, O., Mandrup-Poulsen, T., and Bonny, C. (2000). The c-Jun amino-terminal kinase pathway is preferentially activated by interleukin-1 and controls apoptosis in differentiating pancreatic beta-cells. Diabetes *49*, 1468–1476.

Arkan, M.C., Hevener, A.L., Greten, F.R., Maeda, S., Li, Z.W., Long, J.M., Wynshaw-Boris, A., Poli, G., Olefsky, J., and Karin, M. (2005). IKK-beta links inflammation to obesity-induced insulin resistance. Nat. Med. *11*, 191–198.

Autelli, R., Crepaldi, S., De Stefanis, D., Parola, M., Bonelli, G., and Baccino, F.M. (2005). Intracellular free iron and acidic pathways mediate TNF-induced death of rat hepatoma cells. Apoptosis *10*, 777–786.

Baeyens, L., De Breuck, S., Lardon, J., Mfopou, J.K., Rooman, I., and Bouwens, L. (2005). In vitro generation of insulin-producing beta cells from adult exocrine pancreatic cells. Diabetologia *48*, 49–57.

Berg, D., and Youdim, M.B. (2006). Role of iron in neurodegenerative disorders. Top. Magn. Reson. Imaging *17*, 5–17.

Bonny, C., Nicod, P., and Waeber, G. (1998). IB1, a JIP-1-related nuclear protein present in insulin-secreting cells. J. Biol. Chem. *273*, 1843–1846.

Bradley, B., Prowse, S.J., Bauling, P., and Lafferty, K.J. (1986). Desferrioxamine treatment prevents chronic islet allograft damage. Diabetes *35*, 550–555.

Cai, D., Yuan, M., Frantz, D.F., Melendez, P.A., Hansen, L., Lee, J., and Shoelson, S.E. (2005). Local and systemic insulin resistance resulting from hepatic activation of IKK-beta and NF-kappaB. Nat. Med. *11*, 183–190.

Cappellini, M.D., and Piga, A. (2008). Current status in iron chelation in hemoglobinopathies. Curr. Mol. Med. *8*, 663–674.

Christensen, D.P., Gysemans, C., Dahllof, M.S., Lundh, M., Rasmussen, D.N., Schmidt, S.F., Mandrup, S., Juul, N., Workman, C., Blaabjerg, L., Mascagni, P., Dinarello, C., Billestrup, N., Mathieu, C., Grunnet, L.G., and Mandrup-Poulsen, T. (2011). 477-PP: Inhibition of lysine deacetylase activity protects β-cells from inflammatory attack in vitro and in vivo by targeting NF-κB transcriptional activity. Diabetes *60* (*Supplement 1*), A132.

Cooksey, R.C., Jones, D., Gabrielsen, S., Huang, J., Simcox, J.A., Luo, B., Soesanto, Y., Rienhoff, H., Abel, E.D., and McClain, D.A. (2010). Dietary iron restriction or iron chelation protects from diabetes and loss of beta-cell function in the obese (ob/ob lep-/-) mouse. Am. J. Physiol. Endocrinol. Metab. *298*, E1236–E1243.

Cooksey, R.C., Jouihan, H.A., Ajioka, R.S., Hazel, M.W., Jones, D.L., Kushner, J.P., and McClain, D.A. (2004). Oxidative stress, beta-cell apoptosis, and decreased insulin secretory capacity in mouse models of hemochromatosis. Endocrinology *145*, 5305–5312.

De Souza, C.T., Araujo, E.P., Bordin, S., Ashimine, R., Zollner, R.L., Boschero, A.C., Saad, M.J., and Velloso, L.A. (2005). Consumption of a fat-rich diet activates a proinflammatory response and induces insulin resistance in the hypothalamus. Endocrinology *146*, 4192–4199.

Donath, M.Y., Størling, J., Berchtold, L.A., Billestrup, N., and Mandrup-Poulsen, T. (2008). Cytokines and beta-cell biology: from concept to clinical translation. Endocr. Rev. *29*, 334–350.

Du, F., Qian, Z.M., Zhu, L., Wu, X.M., Yung, W.H., Tsim, T.Y., and Ke, Y. (2009). L-DOPA neurotoxicity is mediated by up-regulation of DMT1-IRE expression. PLoS ONE *4*, e4593.

Eaton, J.W., and Qian, M. (2002). Molecular bases of cellular iron toxicity. Free Radic. Biol. Med. *32*, 833–840.

Eguchi, K., Manabe, I., Oishi-Tanaka, Y., Ohsugi, M., Kono, N., Ogata, F., Yagi, N., Ohto, U., Kimoto, M., Miyake, K., et al. (2012). Saturated fatty acid and TLR signaling link β cell dysfunction and islet inflammation. Cell Metab. *15*, 518–533.

Ehses, J.A., Perren, A., Eppler, E., Ribaux, P., Pospisilik, J.A., Maor-Cahn, R., Gueripel, X., Ellingsgaard, H., Schneider, M.K., Biollaz, G., et al. (2007). Increased number of islet-associated macrophages in type 2 diabetes. Diabetes *56*, 2356–2370.

Eldor, R., Yeffet, A., Baum, K., Doviner, V., Amar, D., Ben-Neriah, Y., Christofori, G., Peled, A., Carel, J.C., Boitard, C., et al. (2006). Conditional and specific NF-kappaB blockade protects pancreatic beta cells from diabetogenic agents. Proc. Natl. Acad. Sci. USA *103*, 5072–5077.

Ellervik, C., Mandrup-Poulsen, T., Andersen, H.U., Tybjærg-Hansen, A., Frandsen, M., Birgens, H., and Nordestgaard, B.G. (2011). Elevated transferrin saturation and risk of diabetes: three population-based studies. Diabetes Care *34*, 2256–2258.

Epsztejn, S., Kakhlon, O., Glickstein, H., Breuer, W., and Cabantchik, I. (1997). Fluorescence analysis of the labile iron pool of mammalian cells. Anal. Biochem. *248*, 31–40.

Friberg, J., Tonnesen, M.F., Heller, S., Pociot, F., Bödvarsdottir, T.B., and Karlsen, A.E. (2010). Inhibition of the nuclear factor-κB pathway prevents

beta cell failure and diet induced diabetes in Psammomys obesus. PLoS ONE *5*, e13341.

Gabutti, V., and Borgna-Pignatti, C. (1994). Clinical manifestations and therapy of transfusional haemosiderosis. Baillieres Clin. Haematol. *7*, 919–940.

Giannoukakis, N., Rudert, W.A., Trucco, M., and Robbins, P.D. (2000). Protection of human islets from the effects of interleukin-1β by adenoviral gene transfer of an Ikappa B repressor. J. Biol. Chem. *275*, 36509–36513.

Gu, G., Dubauskaite, J., and Melton, D.A. (2002). Direct evidence for the pancreatic lineage: NGN3+ cells are islet progenitors and are distinct from duct progenitors. Development *129*, 2447–2457.

Gunshin, H., Fujiwara, Y., Custodio, A.O., Direnzo, C., Robine, S., and Andrews, N.C. (2005). Slc11a2 is required for intestinal iron absorption and erythropoiesis but dispensable in placenta and liver. J. Clin. Invest. *115*, 1258–1266.

Hamazaki, S., Okada, S., Ebina, Y., Fujioka, M., and Midorikawa, O. (1986). Nephrotoxicity of ferric nitrilotriacetate. An electron-microscopic and metabolic study. Am. J. Pathol. *123*, 343–350.

Heimberg, H., Heremans, Y., Jobin, C., Leemans, R., Cardozo, A.K., Darville, M., and Eizirik, D.L. (2001). Inhibition of cytokine-induced NF-kappaB activation by adenovirus-mediated expression of a NF-kappaB super-repressor prevents beta-cell apoptosis. Diabetes *50*, 2219–2224.

Ingrassia, R., Lanzillotta, A., Sarnico, I., Benarese, M., Blasi, F., Borgese, L., Bilo, F., Depero, L., Chiarugi, A., Spano, P.F., and Pizzi, M. (2012). 1B/(-)IRE DMT1 expression during brain ischemia contributes to cell death mediated by NF-κB/RelA acetylation at Lys310. PLoS ONE *7*, e38019.

Jomova, K., and Valko, M. (2011). Importance of iron chelation in free radical-induced oxidative stress and human disease. Curr. Pharm. Des. *17*, 3460–3473.

Kaneto, H., Miyatsuka, T., Shiraiwa, T., Yamamoto, K., Kato, K., Fujitani, Y., and Matsuoka, T.A. (2007). Crucial role of PDX-1 in pancreas development, beta-cell differentiation, and induction of surrogate beta-cells. Curr. Med. Chem. *14*, 1745–1752.

Kekow, J., Ulrichs, K., Müller-Ruchholtz, W., and Gross, W.L. (1988). Measurement of rat insulin. Enzyme-linked immunosorbent assay with increased sensitivity, high accuracy, and greater practicability than established radioimmunoassay. Diabetes *37*, 321–326.

Kurz, T., Gustafsson, B., and Brunk, U.T. (2006). Intralysosomal iron chelation protects against oxidative stress-induced cellular damage. FEBS J. *273*, 3106–3117.

Kwan, E.P., Xie, L., Sheu, L., Ohtsuka, T., and Gaisano, H.Y. (2007). Interaction between Munc13-1 and RIM is critical for glucagon-like peptide-1 mediated rescue of exocytotic defects in Munc13-1 deficient pancreatic beta-cells. Diabetes *56*, 2579–2588.

Larsen, C.M., Wadt, K.A., Juhl, L.F., Andersen, H.U., Karlsen, A.E., Su, M.S.S., Seedorf, K., Shapiro, L., Dinarello, C.A., and Mandrup-Poulsen, T. (1998). Interleukin-1beta-induced rat pancreatic islet nitric oxide synthesis requires both the p38 and extracellular signal-regulated kinase 1/2 mitogen-activated protein kinases. J. Biol. Chem. *273*, 15294–15300.

Larsen, L., Tonnesen, M., Ronn, S.G., Størling, J., Jørgensen, S., Mascagni, P., Dinarello, C.A., Billestrup, N., and Mandrup-Poulsen, T. (2007). Inhibition of histone deacetylases prevents cytokine-induced toxicity in beta cells. Diabetologia *50*, 779–789.

Lehmann, R., Weber, M., Berthold, P., Züllig, R., Pfammatter, T., Moritz, W., Mädler, K., Donath, M., Ambühl, P., Demartines, N., et al. (2004). Successful simultaneous islet-kidney transplantation using a steroid-free immunosuppression: two-year follow-up. Am. J. Transplant. *4*, 1117–1123.

Leiter, E.H. (1982). Multiple low-dose streptozotocin-induced hyperglycemia and insulitis in C57BL mice: influence of inbred background, sex, and thymus. Proc. Natl. Acad. Sci. USA *79*, 630–634.

Leloup, C., Tourrel-Cuzin, C., Magnan, C., Karaca, M., Castel, J., Carneiro, L., Colombani, A.L., Ktorza, A., Casteilla, L., and Pénicaud, L. (2009). Mitochondrial reactive oxygen species are obligatory signals for glucose-induced insulin secretion. Diabetes *58*, 673–681.

Lenzen, S. (2008). Oxidative stress: the vulnerable beta-cell. Biochem. Soc. Trans. *36*, 343–347.

Lenzen, S., Drinkgern, J., and Tiedge, M. (1996). Low antioxidant enzyme gene expression in pancreatic islets compared with various other mouse tissues. Free Radic. Biol. Med. *20*, 463–466.

Li, L., and Frei, B. (2009). Prolonged exposure to LPS increases iron, heme, and p22phox levels and NADPH oxidase activity in human aortic endothelial cells: inhibition by desferrioxamine. Arterioscler. Thromb. Vasc. Biol. *29*, 732–738.

Lundh, M., Christensen, D.P., Damgaard, N.M., Richardson, S.J., Dahllof, M.S., Skovgaard, T., Berthelsen, J., Dinarello, C.A., Stevenazzi, A., Mascagni, P., et al. (2012). Histone deacetylases 1 and 3 but not 2 mediate cytokine-induced beta cell apoptosis in INS-1 cells and dispersed primary islets from rats and are differentially regulated in the islets of type 1 diabetic children. Diabetologia *55*, 2421–2431.

Maedler, K., Størling, J., Sturis, J., Zuellig, R.A., Spinas, G.A., Arkhammar, P.O., Mandrup-Poulsen, T., and Donath, M.Y. (2004). Glucose- and interleukin-1beta-induced beta-cell apoptosis requires Ca2+ influx and extracellular signal-regulated kinase (ERK) 1/2 activation and is prevented by a sulfonylurea receptor 1/inwardly rectifying K+ channel 6.2 (SUR/Kir6.2) selective potassium channel opener in human islets. Diabetes *53*, 1706–1713.

McClain, D.A., Abraham, D., Rogers, J., Brady, R., Gault, P., Ajioka, R., and Kushner, J.P. (2006). High prevalence of abnormal glucose homeostasis secondary to decreased insulin secretion in individuals with hereditary haemochromatosis. Diabetologia *49*, 1661–1669.

Milanski, M., Arruda, A.P., Coope, A., Ignacio-Souza, L.M., Nunez, C.E., Roman, E.A., Romanatto, T., Pascoal, L.B., Caricilli, A.M., Torsoni, M.A., et al. (2012). Inhibition of hypothalamic inflammation reverses diet-induced insulin resistance in the liver. Diabetes *61*, 1455–1462.

Mims, M.P., and Prchal, J.T. (2005). Divalent metal transporter 1. Hematology *10*, 339–345.

Minamiyama, Y., Takemura, S., Kodai, S., Shinkawa, H., Tsukioka, T., Ichikawa, H., Naito, Y., Yoshikawa, T., and Okada, S. (2010). Iron restriction improves type 2 diabetes mellitus in Otsuka Long-Evans Tokushima fatty rats. Am. J. Physiol. Endocrinol. Metab. *298*, E1140–E1149.

Moraes, J.C., Coope, A., Morari, J., Cintra, D.E., Roman, E.A., Pauli, J.R., Romanatto, T., Carvalheira, J.B., Oliveira, A.L., Saad, M.J., and Velloso, L.A. (2009). High-fat diet induces apoptosis of hypothalamic neurons. PLoS ONE *4*, e5045.

Mosley, A.L., and Ozcan, S. (2004). The pancreatic duodenal homeobox-1 protein (Pdx-1) interacts with histone deacetylases Hdac-1 and Hdac-2 on low levels of glucose. J. Biol. Chem. *279*, 54241–54247.

Nanami, M., Ookawara, T., Otaki, Y., Ito, K., Moriguchi, R., Miyagawa, K., Hasuike, Y., Izumi, M., Eguchi, H., Suzuki, K., and Nakanishi, T. (2005). Tumor necrosis factor-alpha-induced iron sequestration and oxidative stress in human endothelial cells. Arterioscler. Thromb. Vasc. Biol. *25*, 2495–2501.

Niederau, C., Fischer, R., Sonnenberg, A., Stremmel, W., Trampisch, H.J., and Strohmeyer, G. (1985). Survival and causes of death in cirrhotic and in noncirrhotic patients with primary hemochromatosis. N. Engl. J. Med. *313*, 1256–1262.

Nielsen, K., Karlsen, A.E., Deckert, M., Madsen, O.D., Serup, P., Mandrup-Poulsen, T., and Nerup, J. (1999). Beta-cell maturation leads to in vitro sensitivity to cytotoxins. Diabetes *48*, 2324–2332.

Nielsen, K., Kruhøffer, M., Orntoft, T., Sparre, T., Wang, H., Wollheim, C., Jørgensen, M.C., Nerup, J., and Karlsen, A.E. (2004). Gene expression profiles during beta cell maturation and after IL-1beta exposure reveal important roles of Pdx-1 and Nkx6.1 for IL-1beta sensitivity. Diabetologia *47*, 2185–2199.

Nomikos, I.N., Prowse, S.J., Carotenuto, P., and Lafferty, K.J. (1986). Combined treatment with nicotinamide and desferrioxamine prevents islet allograft destruction in NOD mice. Diabetes *35*, 1302–1304.

Ortis, F., Cardozo, A.K., Crispim, D., Störling, J., Mandrup-Poulsen, T., and Eizirik, D.L. (2006). Cytokine-induced proapoptotic gene expression in insulin-producing cells is related to rapid, sustained, and nonoscillatory nuclear factor-kappaB activation. Mol. Endocrinol. *20*, 1867–1879.

Paradkar, P.N., and Roth, J.A. (2006a). Nitric oxide transcriptionally down-regulates specific isoforms of divalent metal transporter (DMT1) via NF-kappaB. J. Neurochem. *96*, 1768–1777.

Paradkar, P.N., and Roth, J.A. (2006b). Post-translational and transcriptional regulation of DMT1 during P19 embryonic carcinoma cell differentiation by retinoic acid. Biochem. J. *394*, 173–183.

Persson, H.L., Yu, Z., Tirosh, O., Eaton, J.W., and Brunk, U.T. (2003). Prevention of oxidant-induced cell death by lysosomotropic iron chelators. Free Radic. Biol. Med. *34*, 1295–1305.

Rajpathak, S.N., Crandall, J.P., Wylie-Rosett, J., Kabat, G.C., Rohan, T.E., and Hu, F.B. (2009). The role of iron in type 2 diabetes in humans. Biochim. Biophys. Acta *1790*, 671–681.

Salazar, J., Mena, N., Hunot, S., Prigent, A., Alvarez-Fischer, D., Arredondo, M., Duyckaerts, C., Sazdovitch, V., Zhao, L., Garrick, L.M., et al. (2008). Divalent metal transporter 1 (DMT1) contributes to neurodegeneration in animal models of Parkinson's disease. Proc. Natl. Acad. Sci. USA *105*, 18578–18583.

Szklarczyk, D., Franceschini, A., Kuhn, M., Simonovic, M., Roth, A., Minguez, P., Doerks, T., Stark, M., Muller, J., Bork, P., et al. (2011). The STRING database in 2011: functional interaction networks of proteins, globally integrated and scored. Nucleic Acids Res. *39* (Database issue), D561–D568.

Telfer, J.F., and Brock, J.H. (2002). Expression of ferritin, transferrin receptor, and non-specific resistance associated macrophage proteins 1 and 2 (Nramp1 and Nramp2) in the human rheumatoid synovium. Ann. Rheum. Dis. *61*, 741–744.

Telfer, J.F., and Brock, J.H. (2004). Proinflammatory cytokines increase iron uptake into human monocytes and synovial fibroblasts from patients with rheumatoid arthritis. Med. Sci. Monit. *10*, BR91–BR95.

Tiedge, M., Lortz, S., Drinkgern, J., and Lenzen, S. (1997). Relation between antioxidant enzyme gene expression and antioxidative defense status of insulin-producing cells. Diabetes *46*, 1733–1742.

Tonnesen, M.F., Grunnet, L.G., Friberg, J., Cardozo, A.K., Billestrup, N., Eizirik, D.L., Størling, J., and Mandrup-Poulsen, T. (2009). Inhibition of nuclear factor-kappaB or Bax prevents endoplasmic reticulum stress- but not nitric oxide-mediated apoptosis in INS-1E cells. Endocrinology *150*, 4094–4103.

Vaithilingam, V., Oberholzer, J., Guillemin, G.J., and Tuch, B.E. (2010). Beneficial effects of desferrioxamine on encapsulated human islets—in vitro and in vivo study. Am. J. Transplant. *10*, 1961–1969.

Wang, H., Iezzi, M., Theander, S., Antinozzi, P.A., Gauthier, B.R., Halban, P.A., and Wollheim, C.B. (2005). Suppression of Pdx-1 perturbs proinsulin processing, insulin secretion and GLP-1 signalling in INS-1 cells. Diabetologia *48*, 720–731.

Wang, H., Maechler, P., Ritz-Laser, B., Hagenfeldt, K.A., Ishihara, H., Philippe, J., and Wollheim, C.B. (2001). Pdx1 level defines pancreatic gene expression pattern and cell lineage differentiation. J. Biol. Chem. *276*, 25279–25286.

Warren, S., Torti, S.V., and Torti, F.M. (1993). The role of iron in the cytotoxicity of tumor necrosis factor. Lymphokine Cytokine Res. *12*, 75–80.

Wicksteed, B., Brissova, M., Yan, W., Opland, D.M., Plank, J.L., Reinert, R.B., Dickson, L.M., Tamarina, N.A., Philipson, L.H., Shostak, A., et al. (2010). Conditional gene targeting in mouse pancreatic ß-Cells: analysis of ectopic Cre transgene expression in the brain. Diabetes *59*, 3090–3098.

Witzleben, C.L. (1966). An electron microscopic study of ferrous sulfate induced liver damage. Am. J. Pathol. *49*, 1053–1067.

Yu, Z., Persson, H.L., Eaton, J.W., and Brunk, U.T. (2003). Intralysosomal iron: a major determinant of oxidant-induced cell death. Free Radic. Biol. Med. *34*, 1243–1252.

Yuan, M., Konstantopoulos, N., Lee, J., Hansen, L., Li, Z.W., Karin, M., and Shoelson, S.E. (2001). Reversal of obesity- and diet-induced insulin resistance with salicylates or targeted disruption of Ikkbeta. Science *293*, 1673–1677.

Zalzman, M., Anker-Kitai, L., and Efrat, S. (2005). Differentiation of human liver-derived, insulin-producing cells toward the beta-cell phenotype. Diabetes *54*, 2568–2575.

Zalzman, M., Gupta, S., Giri, R.K., Berkovich, I., Sappal, B.S., Karnieli, O., Zern, M.A., Fleischer, N., and Efrat, S. (2003). Reversal of hyperglycemia in mice by using human expandable insulin-producing cells differentiated from fetal liver progenitor cells. Proc. Natl. Acad. Sci. USA *100*, 7253–7258.

Zhang, X., Haaf, M., Todorich, B., Grosstephan, E., Schieremberg, H., Surguladze, N., and Connor, J.R. (2005). Cytokine toxicity to oligodendrocyte precursors is mediated by iron. Glia *52*, 199–208.

Zhang, X., Zhang, G., Zhang, H., Karin, M., Bai, H., and Cai, D. (2008). Hypothalamic IKKbeta/NF-kappaB and ER stress link overnutrition to energy imbalance and obesity. Cell *135*, 61–73.